Computer Engineering and Intelligent Systems
ISSN 2222-1719 (Paper) ISSN 2222-2863 (Online)
Vol.7, No.2, 2016
www.iiste.org

Ear Symmetry Evaluation on Selected Feature Extraction Algorithms in Ear Biometrics

Adeolu Afolabi Ademiluyi Desmond
Department of Computer Science and Engineering, Ladoke Akintola University of Technology, Ogbomosho, Oyo State, Nigeria

Abstract
The human ear has an intriguing shape and like most parts of the human body, bilateral symmetry is observed between left and right. Occlusions of the ear is a major problem in ear recognition, however, if ear symmetry is established, then reconstructing partially occluded ear images will be possible from the other ear, also the left ear of an individual's test image can be matched against the right ear in the gallery database (or vice-versa). This paper presented an evaluation of the relationship between left and right ear using four selected feature extraction algorithms: Principal Component Analysis (PCA), Speeded Up Robust Features (SURF), Geometric feature extraction and Gabor wavelet based feature extraction techniques in terms of performance issues given by of False Acceptance Rate (FAR), False Rejection Rate (FRR), and Genuine Acceptance Rate (GAR).The approach was evaluated on non-public ear dataset and simulated in MATLAB Environment. For these selected feature extraction algorithms, the right ears of the subjects are used as the gallery, and the left ear as the probe. The experimental results suggest the existence of some degree of symmetry in the human ears but the ear are not exactly identical as the recognition accuracy of the system declined for three (PCA, SURF, and Gabor wavelet) of the feature extraction algorithms, FRR rising to over 84% for SURF. However, Geometric feature extraction reported relatively high recognition accuracy with FRR of 12.50% and GAR of 87.50%.
Keywords: Ear symmetry, Gabor wavelet, Occlusion, Principal Component Analysis (PCA), Speeded Up Robust Features (SURF).

Introduction

Ear based recognition is of particular interest because unlike face recognition it is not affected by factors such as mood or health. Significantly, the appearance of the outer ear is nearly unaffected by aging (Iannarelli, 1989), making ear better suited for long-term identification when compared to other non-invasive techniques such as face recognition. The potential for using the ear's appearance as a means of personal identification was recognized and advocated as early as 1890 by the French criminologist Alphonse Bertillon (Bertillon, 1890).

Human ears are located on both sides of the face and, therefore, the issue of symmetry of the structure of the two ears is a subject of interest. Such an analysis has several implications in a practical recognition system. One, if symmetry is established, then the left ear of an individual's probe image can be matched against their right ear in the gallery database (or vice-versa). Secondly, occlusion is a major problem in Ear recognition, reconstructing partially occluded ear images will be possible, if information about the other ear is available. Third, if the ears of an individual are greatly asymmetrical, then this provides additional information about their identity (Abaza *et al.,* 2010).

The study of Ear began with the work of Iannarelli (Iannarelli, 1989) where ear was claimed to be unique to each individual. The Ear was further classified by dividing it into seven parts as shown in Figure 1. Medical reports have shown that the variation over time in ear is most noticeable during the period from four months to eight years old and over 70 years old (Li *et al.*, 2015). Due to the ear's stability and predictable changes, ear features are potentially a promising biometric for use in a human identification (Bhanu *et al*., 2003). Burge *et al.* (Burge *et al.,* 2000) also studied the possibility of automated ear recognition. The method localized the ear in an image by using deformable contours on a Gaussian pyramid representation of the gradient image. Afterwards, a sequence o edge extraction and curve extraction techniques were used to build a graph model of the ear. A graph matching technique was used to assess the similarity of two ears. Moreno and Sanchez (Moreno *et al.,* 1999) describe a fully automated ear recognition system. The system relied on multiple features pertaining to the contour of the outer ear, and the shape and wrinkle information contained in the ear image to establish identity.

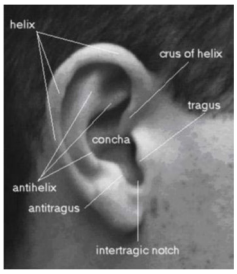

Figure 1: Anatomy of an ear (Dasari, 2006).

Methodology
The system was designed using MATLAB R2013a programming Environment. The choice of the design environment is based on the availability of image processing applications.

Data Collection
Over 500 non public ear images were collected using Tecno P9 Camera in the same lightening conditions with no illumination changes. The images were carefully taken from the right side of the face to preserve the outer ear shape with a distance of 15-20 cm [6] between the face and the camera. These images are used for training the automatic ear detector and for recognition.

The Proposed Ear Recognition System
The proposed Ear Recognition System is divided into five major steps- Image acquisition, Edge detection and normalization, Feature extraction, Feature selection and Ear recognition. Fig. 2 shows a proposed flow diagram for the ear recognition system.

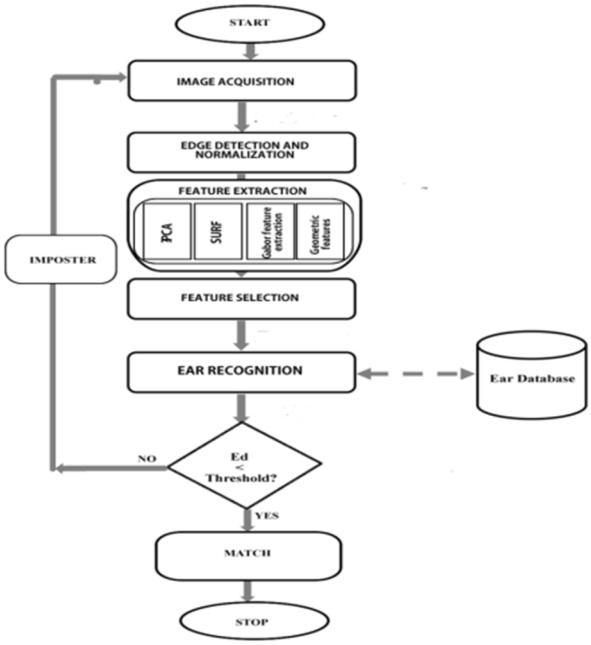

Figure 2: Flowchart of the proposed Ear Recognition System.

Image Acquisition
The side image is acquired from a system's web camera using the webcam object in Matlab. The webcam object connects to the camera establishing exclusive access and starts streaming. The image is then previewed and acquired using the Matlab snapshot function.

Edge Detection and Normalization
The Region of Interest (ROI) in this research work is the Ear; which is detected by trained a cascade detector in Matlab. After the ROI selection, the image is converted to grayscale and the edge detection is done using the canny edge detector [7]. Median filter is used to remove noises and Standard deviation computation is made to enhance the dimension of the output image so that it helps to detect edges clearly. Normalization is done by considering the Ear image estimated mean (M) and variance (v). The input image I (x, y) is normalized by using the equations:

$N_i(x, y) = M_0 + \sqrt{\frac{(V_0 * I(x,y) - M_i)^2}{V_i}}$; if $I(x, y) \geq M$ (1)

$N_i(x, y) = M_0 - \sqrt{\frac{(V_0 * I(x,y) - M_i)^2}{V_i}}$; otherwise (2)

Feature Extraction

After completion of ROI selection, enhancement and normalization operations, the images are ready for feature extraction. The Concha is taken as the local feature and Outer Helix is taken as the global part of ear image. In this proposed approach, four key feature extraction techniques are used. The four feature extraction algorithms are selected based on their rank-1 performance as shown from the work of Anika *et al.* [8]. The four feature extraction algorithms considered in this research work are:

1. Principal Component Analysis (PCA)
2. Speeded Up Robust Feature (SURF) Transform
3. Gabor wavelet based feature extraction
4. Geometric features

Principal Component Analysis (PCA)

The 'principal components' are obtained by the Eigen decomposition of the covariance matrix of the ear data, the dimensionality is then reduced by finding a linear subspace of the original feature space on to which the ear data is projected such that the projection error is minimized. Each image's pixels are taken row by row from top to bottom and converted to a row vector containing the gray scale or intensity values of that image. These row vectors are then concatenated in a single matrix so that each row in that matrix corresponds to an image. This process is done to training images as well as test images, keeping them in two separate matrices.

The covariance matrix is then calculated for the training images where each row represents an image (observation) and each column represent a pixel position (variable). Covariance is the measure of how much two variables vary together which is calculated using the following formula:

$cov(x_i,x_j) = E((x_i - \mu_i)(x_j - \mu_j))$ For i and j = 1,2,....,*n* (3)

where *E* is the mathematical expectation and $\mu_i = Ex_i$, and *x* is the training images matrix. If the size of *x* is (*m* x *n*), where *m* is the number of images (rows) and *n* is the number of pixels per image (columns), then the resulting covariance matrix (*C*) will be of size (*n* x *n*). If the covariance matrix (*C*) satisfies the relation $Ce_i = \lambda_i e_i$; where λ_i and e_i for i=1,2…,n are the corresponding eigenvectors and eigenvalues respectively then matrix *A* from the eigenvectors sorted by decreasing eigenvalues is constructed.

Speeded Up Robust Feature Transform Features (SURF)

There are two important steps involved in extracting SURF features from an Ear image. These are finding key-points and computation of their respective descriptor vectors.

SURF makes use of hessian matrix for key-point detection. For a given point P(x; y) in an image I, the hessian matrix is defined as:

$$H(P,\sigma) = \begin{bmatrix} Lxx(P,\sigma) & Lxy(P,\sigma) \\ Lyx(P,\sigma) & Lyy(P,\sigma) \end{bmatrix} \quad (4)$$

Where Lxx(P,σ), Lxy(P,σ), Lyz(P,σ) and Lyy(P,σ) are the convolution of the Gaussian second order derivatives $\frac{\partial^2}{\partial x^2}g(\sigma)$, $\frac{\partial^2}{\partial x \partial y}g(\sigma)$, $\frac{\partial^2}{\partial x \partial y}g(\sigma)$, and $\frac{\partial^2}{\partial y^2}g(\sigma)$, with the image I at point P respectively.

In order to generate the descriptor vector of a key-point, a circular region is considered around each detected key-points and Haar wavelet responses dx and dy in horizontal and vertical directions are computed.

Gabor feature extraction

For extracting features with Gabor filters, each point in the ear image is represented by local Gabor filter responses. A 2-D Gabor filter is obtained by modulating a 2-D sine wave with a Gaussian envelope. The 2-D Gabor filter kernel is defined by:

$$f(x, y, \theta_k, \lambda) = \exp\left[-\frac{1}{2}\left\{\frac{(x\cos\theta_k + y\sin\theta_k)^2}{\sigma_x^2} + \frac{(-x\sin\theta_k + y\cos\theta_k)^2}{\sigma_y^2}\right\}\right] . \exp\left\{\frac{2\pi(x\cos\theta_k + y\sin\theta_k)}{\lambda} i\right\} \quad (5)$$

where σ_x and σ_y are the standard deviations of the Gaussian envelope along the *x* and *y*-dimensions, respectively. λ and θ_k are the wavelength and orientation, respectively. The spread of the Gaussian envelope is

defined using the wavelength λ. A rotation of the $x - y$ plane by an angle θ_k result in a Gabor filter at orientation θ_k. θ_k is defined by:

$$\theta_k = \frac{\pi}{n}(k - 1) \qquad k = 1, 2, .., \ n \tag{6}$$

where n denotes the number of orientations. The Gabor local feature at a point (X,Y) of an image can be viewed as the response of all different Gabor filters located at that point. A filter response is obtained by convolving the filter kernel (with specific λ, θ_k) with the image. Gabor kernels with 8 orientation and 4 scales/wavelengths was used. For sampling point (X,Y), the Gabor filter response, denoted as g(.), is defined as:

$$g(X, Y, \theta_k, \lambda) = \sum_{x=-X}^{N-X-1} \sum_{y=-Y}^{N-Y-1} I(X + x, Y + y) f(x, y, \theta_k, \lambda) \tag{7}$$

where $I(x,y)$ denotes an NxN greyscale image. Gabor filters at multiple frequencies (λ) and orientations (θ_k) was applied at a specific point (X,Y) which produces a set of filter responses for that point, denoted as a Gabor jet. A jet J is defined as the set $\{J_j\}$ of complex coefficients obtained from one image point, and can be written as:

$$J_j = a_j \exp(i\phi_j) \quad j=1,..,n \tag{8}$$

where a_j is magnitude and ϕ_j is phase of Gabor features/coefficients.

Geometrical Method of Feature Extraction

A 2 step concentric geometrical methods of feature extraction based on numbers of pixels that have the same radius in a circle with the centre in the centroid and on the contour topology was used. The algorithm [9] for the feature extraction is presented below:

Step 1: A set of circles with the centre in the centroid is created.
Step 2: Number of circles N_r is fixed and unchangeable.
Step 3: Corresponding radiuses are α pixels longer from the previous radius.
Step4: Since each circle is crossed by the contour image pixels, the number of intersection pixels *lr* is counted.
Step 5: All the distances *d* between neighboring pixels is counted in a counter clockwise direction.
Step 6: The feature vector that consists of all the radiuses with the corresponding number of pixels belonging to each radius are built and sum of all the distances between those pixels Σ*d* are calculated.

Features Selection

The Sequential Floating Forward Selection method (SFFS) was used in order to select the most relevant and discriminating subset of features from the initial one and get rid of the redundant features. The SFFS algorithm is described by the following pseudocode:

1. Initialize feature to empty subset Y = {θ};
2. Find the best feature and update Y_m(*forward*)
   X+= argmin (J(Yk+x))
   AεYk
   $Y_{k+1}=Y_k + X^+$
   K= k+1
3. Find the worst feature(backward)
   x^- = argmin (J(Yk + x))
   aε Y_k
4. If $J(Y_k - x^-) < J(Y_k)$ then
   $Y_{k+1} = Y_k - X^-$
   K=k-1
   Go to step 4
   else
   Go to step 3
   End if

Ear Database

The ear database consists of 144 Ear samples taken from 72 subjects along with other attributes like name, physical identity and generated results of the processed images. Sample ear images from database are shown in Fig. 3.

Figure 3: Sample Ear images from database

Ear Recognition

For successful identification, the system compiles the inter-distance based on the image biometrics for both training images and test images and then compares the inter-distance, the inter-distance *D* is given by:

$$D=\sqrt{(X_1 - X_2)^2 + (Y_2 - Y_2)^2} \quad (9)$$

(X_1, X_2) and (Y_2, Y_2) are coordinates of two intersections.

The Euclidean distance *ED* is then calculated using the following formula:

$$ED = \sqrt{(D_T - D_{db})^2} \quad (10)$$

Where D_T and D_{db} are the test and database ear pattern inter-distances.

The algorithm for the matching is presented below:

1. To match two images (one test image T with another from the database db)
   The Euclidean distance between the two weight matrices of those images is calculated.
2. A test run of the system is used to set a threshold.
3. If the Euclidean distance is higher than a threshold, the output is an imposter, otherwise system outputs a match.

Performance Evaluation and Analytical Technique

A GUI is created in Matlab as shown in Fig. 4 for entering and identification of a person. The system is then serially presented with 72 genuine subjects and a set of 72 imposters using each feature extraction algorithm. Four experiments with different parameters altered were then carried out. A quantifiable assessment of the accuracy and other characteristics of the system are then measured using performance metrics: False Acceptance Rate (FAR), False Rejection Rate (FRR), Genuine Acceptance Rate (GAR), and Recognition Accuracy.

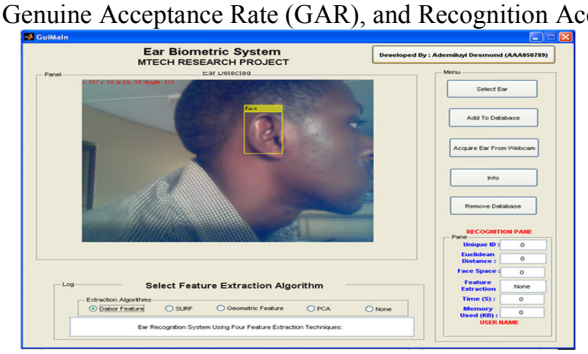

Figure 4: The Developed Ears Recognition System

Ear Symmetry Experiment

Table 1: Performance Analysis of PCA Feature Extraction Algorithm for Recognition using the Left Ear

Genuine Users	Number of Users	Total Matches (Attempt)			FRR (%)			GAR (%)		
		1st	2nd	3rd	1st	2nd	3rd	1st	2nd	3rd
Right Ear	72	68	70	70	4.16	2.77	2.77	95.84	97.23	97.23
Left Ear	72	42	29	33	41.67	59.72	54.16	58.33	40.28	45.84

Table 2: Performance Analysis of Gabor Feature Extraction Algorithm for Recognition using the Left Ear

Users	Number of Users	Total Matches (Attempt)			FRR (%)			GAR (%)		
		1st	2nd	3rd	1st	2nd	3rd	1st	2nd	3rd
With Right Ear	72	69	70	69	4.16	2.78	4.16	95.84	97.22	95.84
With Left Ear	72	29	42	37	59.72	41.67	48.61	40.28	58.33	51.39

Table 3: Performance Analysis of Geometric Feature Extraction Algorithm for Recognition using the Left Ear

Genuine Users	Number of Users	Total Matches (Attempt)			FRR (%)			GAR (%)		
		1st	2nd	3rd	1st	2nd	3rd	1st	2nd	3rd
Right Ear	72	60	68	68	16.67	5.56	5.56	83.33	94.44	94.44
Left Ear	72	63	51	60	12.50	29.17	16.67	87.50	70.83	83.33

Table 4: Performance Analysis of SURF Feature Extraction Algorithm for Recognition using the Left Ear

Genuine Users	Number of Users	Total Matches (Attempt)			FRR (%)			GAR (%)		
		1st	2nd	3rd	1st	2nd	3rd	1st	2nd	3rd
Right Ear	72	65	67	65	9.72	6.94	9.72	90.28	93.06	90.28
Left Ear	72	11	19	22	84.72	73.62	69.44	15.28	25.38	30.56

Discussion

The right ear of the subject is used as the gallery, and the left is used as the probe. For the four feature extraction algorithms, the subjects made attempts at recognition using both ears. The results are presented in Table 1, Table 2, Table 3, and Table 4.

Table1 shows the performance analysis of the recognition system when PCA was used as the feature extraction algorithm for the left ear. The recognition accuracy significantly fell with the system obtaining FRR of 41.67%, 59.72% and 59.72% respectively; these high values of FRR indicate a serious decline in the performance of the system compared to FRR values of 4.16%, 2.72% and 2.77% obtained for the right ear. The GAR values crashed from 95.84%, 97.23% and 97.23% for the right ear to 58.33%, 40.26% and 45.84% respectively for the left ear.

Table 2 reflects the Ear biometric system performance with Gabor feature extraction technique. The results obtained indicated that the left and right ear image are not exactly alike as the system obtained very unfavorable values of FRR of 59.72%, 41.67% and 48.61% resulting in GAR decline with reported values of 40.28%, 58.30% and 51.39% respectively during the three attempts at recognition with the left ear.

Table 3 shows the performance of the biometric system with Geometric feature extraction for left ear. The system obtained FRR of 12.50%, 29.17% and 16.67% respectively, this FRR values are considerable low suggesting that Geometric feature extraction technique is good when comparing left and right ear patterns. The GAR values obtained for the left ear were reasonable high at 87.50%, 70.83% and 83.33% respectively, comparing fairly well with GAR of 83.33%, 94.44% and 94.44% obtained for the right ear.

In Table 4 is the performance analysis of the system for SURF feature extraction on left ear recognition. The calculated FRR were 84.72%, 73.62% and 69.44%, these high values of FRR indicated a very low performance of the recognition system. For instance, only 11 genuine subjects were correctly identified from a pool of 72 genuine subjects at the first attempt with SURF feature extraction. This type of result is unacceptable; hence SURF falls short on left ear recognition. Figure 5 shows the Genuine Acceptance Rate of the feature

extraction algorithms for both ears.

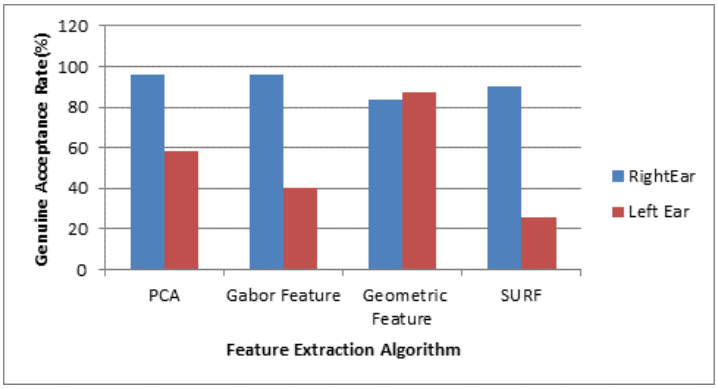

Figure 5: Acceptance Rate for Both Ears Using the Four Algorithms

Conclusion and Future Work

This paper attempted to analyze the symmetry of the two ears by examining the performance of the ear biometric system using four feature extraction algorithms. The experimental results suggest the existence of some degree of symmetry in the human ears but the ears are not exactly identical as the performance of the system fell for three (PCA, Gabor, and SURF) of the four feature extraction algorithms, FRR rose to over 84% with SURF. However, Geometric feature extraction reported favorable GAR values with the left ear, recognizing 63 genuine subjects from a total of 72 genuine subjects at the first attempt, obtaining a FRR of 12.5% and GAR of 87.50%. The overall result obtained with Geometric feature extraction showed promising results for left ear matching. However, a larger dataset is needed to verify these results; future work could look into designing parametric models for the ear edges and using them to quantify the symmetry of individual ear parts.

References

Abaza A. and Arun R. (2010). 'Towards Understanding the Symmetry of Human Ears: A Biometric Perspective'. In: Proc. of 4th IEEE International Conference on Biometrics: Theory, Applications and Systems (BTAS), (Washington DC, USA), pp. 1 -6.

Abaza A. Hebert C. and Harrison MAF. (2010). 'Fast Learning Ear Detection for Real-time Surveillance'. In: Fourth IEEE International Conference on Biometrics: Theory Applications and Systems (BTAS), pp. 1 -6.

Anika P, and Christoph B. (2012) July. Ear Biometrics: A Survey of Detection, Feature Extraction and Recognition Methods. Institute of Engineering and Technology.; 2(4):718 -737.

Bertillon A. (1980), La Photographie Judiciaire, avec un Appendice sur la Classification et l'Identification Anthropometriques, Gauthier-Villars, Paris, pp. 12-19.

Bhanu B. and Chen H. (2003). Human ear recognition in 3D. In Workshop on Multimodal User Authentication, pp. 91–98.

Burge M, and Burger W. (2000) "Ear Biometrics in Computer Vision," 15th International Conference of Pattern Recognition (ICPR), pp. 826–830.

Canny J. (1986). A Computational Approach to Edge Detection, IEEE Trans. on Pattern Analysis and Machine Intelligence, 8(6): 679-698.

Chang K, Bowyer K, Sarkar K, and Victor B, "Comparison and Combination of Ear and Face Images in Appearance-Based Biometrics," IEEE Transactions on Pattern Analysis and Machine

Choras M. (2008). 'Perspective Methods of Human Identifiication: Ear Biometrics'. Opto- Electronics Review.16(1):85-96.

Dasari N, (2006). A Simple Geometric Approach for Ear Recognitiomn. Graduate Progra in Department of Computer Science and Engineering Indian Institute of Technology, Kanpur India, pp. 1321- 1331

Iannarelli A. (1989). Ear Identification. Paramont Publishing Company. pp. 1 -12.

Li B, and Chang T. (2015) Ear Biometric in 2D images, Institute of Ear Biometric Research (IEBR) Journal, *15(3):* 169-181.

Moreno B, and Sanchez A. (1999) "On the Use of Outer Ear Images for Personal Identification in Security Applications," in the 33rd International Conference on Security Technology. pp. 469-476.